Optimizing GaAs nanowire-based visible-light photodetectors

View Online   Export Citation   CrossMark

Xiao Li,[1,2] (iD) Xuezhe Yu,[1,a)] Haotian Zeng,[1] Giorgos Boras,[1] Kai Shen,[1,2] Yunyan Zhang,[1] Jiang Wu,[2] (iD)
Kwang Leong Choy,[3,a)] and Huiyun Liu[1,a)]

AFFILIATIONS

[1]Department of Electronic and Electrical Engineering, University College London, London WC1E 7JE, United Kingdom
[2]Institute of Fundamental and Frontier Sciences, University of Electronic Science and Technology of China, Chengdu 610054,
  People's Republic of China
[3]Institute for Materials Discovery, University College London, Roberts Building, Malet Place, London WC1E 7JE, United Kingdom

[a)]Authors to whom correspondence should be addressed: xuezhe.yu@ucl.ac.uk; k.choy@ucl.ac.uk; and huiyun.liu@ucl.ac.uk

ABSTRACT

Sole surface passivation for III–V nanowire photodetectors exhibits limited photoresponse improvement. Consequently, a well-customized contact design is crucial. Here, GaAs nanowire-based metal-semiconductor-metal photodetectors via surface treatment and interfacial contact optimization are reported. The passivation strategy inhibits the surface recombination and, importantly, effectively reduces the Fermi-level pinning effect by the redistribution of surface states. It leads to the Schottky barrier height reduced from $\sim$0.63 to $\sim$0.36 eV at the Ni/GaAs nanowire contact. The design contributes to the prominently enhanced more than tenfold photoresponsivity and the much-shortened response time, in comparison with the pristine ones. When applying the design to the intrinsic GaAs nanowire photodetector, it demonstrates a responsivity of 4.5×10^4 A/W, a specific detectivity of 3.3×10^{14} Jones, and response time less than 50 ms under 520 nm laser illumination. Additionally, good repeatability of dynamic photo-switching characteristics and stability measured with slight degradation after 2 months are demonstrated. With the same approach, it is found that the responsivity could be further enhanced by over 50 times up to 6.4×10^5 A/W via fermi level adjustment in a p-doped single GaAs nanowire device. Featuring the nanoscale footprint and compact size, the results establish the GaAs nanowire as a promising and competitive candidate for high-performance and reliable nano-photodetection operating in the visible range.

Owing to the tunable bandgap, the large surface-to-volume ratio as well as the strong light–matter interaction, III–V nanowires (NWs) have been exploited for a broad range of optoelectronic applications such as photodetectors,[1,2] solar cells,[3,4] lasers,[5,6] and light-emitting diodes.[7] Among them, nanowire-based photodetectors have been the topic of extensive research as promising building blocks in nanophotonics.[8–10] In order to meet the increased demands and up-to-date requirements regarding the research and applicability of these devices, photodetectors exhibiting high responsivity and demonstrating capability for weak signal detection are highly desired.[11–13]

As a representative direct-bandgap conventional III–V semiconductor, GaAs (a bandgap of 1.42 eV) absorbs light efficiently, resulting in superior photoresponse performance in different structures[2,14–19] and with the incorporation of 2D materials.[20,21] While the achievements reported up-to-date are impressive, GaAs NW-based photodetectors are severely affected by the surface states, especially the high surface

recombination velocity up to 5.4×10^5 cm/s.[22] The high density of surface states acts as non-radiative carrier traps and scattering centers, thus degrading GaAs nanowire photodetector characteristics. Consequently, the reduction of surface states via surface passivation allows longer lifetimes and less scattering of the photoinduced carriers. Especially, sulfur passivation using ammonium sulfide $(NH_4)_2S$ solution has been proved to effectively suppress the surface recombination and lead to higher minority carrier diffusion lengths[23] by providing S-ions to saturate the dangling bonds for GaAs NWs.[24–26]

However, surface passivation does not seem to necessarily lead to significant enhancement of the photodetection performance, while the ratio of photoluminescence (PL) intensity enhancement is often more than tenfold.[1,25,27] For instance, mere sulfur passivation increases the responsivity from 18.2 to 25 A/W in the GaAs nanowire device with Cr/Au contacts,[24] while a single $GaAs_xSb_{1-x}$/InP core/shell NW photodetector shows a responsivity of 325.1 A/W, compared to a

corresponding value of 143.5 A/W for the core-only counterpart.[28] The contact in the photoelectric conversion process plays a critical role particularly in Schottky-junction detectors and metal-semiconductor-metal (MSM) detectors.[29,30] Hence, opposite to the non-contacted optically excited measurements, the introduction of contacts in photoresponse measurements often complicates the accomplishment of the surface passivation effect due to the altered features of the interfaces. Therefore, in addition to an effective passivation technique, a well-customized contact structure is also indispensable and should be taken into account jointly in the design. Despite this fact, the synergic influences of these factors have not been considered so far for passivated photodetectors in the majority of studies.

In this report, photodetectors based on GaAs NWs are demonstrated via hybrid surface passivation and interfacial contact optimization. Sulfur treatment produces an approximate 9.5-fold increase in the PL intensity as well as evidence of surface passivation. The Schottky barrier height is reduced from ~ 0.63 to ~ 0.36 eV at the Ni/GaAs nanowire contact after passivation. The optimized intrinsic GaAs nanowire device shows a significantly enhanced photoresponse, including a high responsivity of 4.5×10^4 A W^{-1}, specific detectivity reaching up to 3.3×10^{14} Jones, and short response time less than 50 ms upon 520 nm laser illumination. With the same treatment, the responsivity is further enhanced by over 50-time in the p-doped GaAs nanowire device, up to 6.4×10^5 A/W. Furthermore, the hybrid design is demonstrated to improve the photoresponse performance with good reliability and stability.

GaAs NWs were synthesized by molecular beam epitaxy (MBE) via the self-catalyzed vapor−liquid−solid technique to avoid foreign impurities, which severely degrade the material optoelectronic characteristics.[31,32] Initially, an intrinsic zinc blende GaAs nanowire structure with low density of defects was employed as the active channel material.[31] The lengths of NWs were typically within the range of 10–20 μm, and the diameters varied from 150 to 180 nm. The surface treatment using ammonium sulfide (NH$_4$)$_2$S solution was applied on GaAs NWs. The schematic image of a back-gate single nanowire device is displayed in Fig. 1(a). Atomic force microscopy (AFM) image of a passivated intrinsic GaAs nanowire is shown in Fig. 1(b), revealing good uniformity and the diameter of $\sim$150 nm. The scanning electron microscope (SEM) image and the optical image of the same device are shown in Figs. S1(a) and S1(b), respectively. Other characterization results including the SEM image of as-grown GaAs NWs and the

AFM image of single intrinsic GaAs nanowire device are present in Figs. S2(a) and S2(b), respectively.

To identify the reduction of the surface recombination, the PL spectra were measured under 532 nm illumination at room-temperature. As shown in Fig. 2(a), both GaAs nanowire samples exhibited a PL peak at 870.4 nm arising from interband optical transition in the nanowire materials. Approximately a 9.5-fold increase in the peak intensity for the passivated sample was observed, suggesting efficient enhancement of radiative recombination rate in the NWs. The schematic energy band diagram is illustrated in Fig. 2(b) with the change in the Schottky barrier heights indicated. It is worth mentioning that the intrinsic GaAs nanowires used here are weakly p-doped, which might be due to an unintentional doping in the growth reactor or the formation of anti-site defects, where Ga occupies As position.[14,16] Owing to the surface states of GaAs nanowires, the Fermi-level position at the surface is pinned at an energy level, which is essentially almost independent of the metal.[24,33] According to the measured temperature dependent I-V relationship as shown in Fig. 2(c), the barrier height of ~ 0.63 eV at the Ni/GaAs nanowire contact was extracted for the pristine device [Figs. S3(a)–S3(b)], as explained in the supplementary material.

The sulfur passivation renders the Schottky barrier height re-determined by the redistribution of surface states. In a similar way, the barrier height of ~ 0.36 eV was calculated for the contact between Ni and the passivated GaAs nanowire [Figs. 2(d), S3(c), and S3(d)]. Therefore, the formation of the Ni/GaAs nanowire contact allows more efficient carrier collection driven by the lower barrier height, and as a result, both the dark current and the photocurrent could be amplified. Although the dark current is increased, the intrinsic nature of the structure will impede its excessive enhancement. Consequently, an optimized design is expected from the trade-off between the dark current and the photocurrent. The employment of high-quality GaAs NWs, the efficient surface passivation, and the designed lowered Schottky barrier height at the contact contribute to the optimization of the devices toward high-performance GaAs nanowire photodetectors.

Figures 3(a) and S4 illustrate the output and transfer characteristics of a passivated device in the dark, respectively. With the increase in the back-gate voltage, the drain-source current I$_{DS}$ slightly dropped, indicating the weak p-type property. Subsequently, the photoresponse of the passivated GaAs nanowire photodetector in a MSM structure was systematically characterized under visible light illumination.
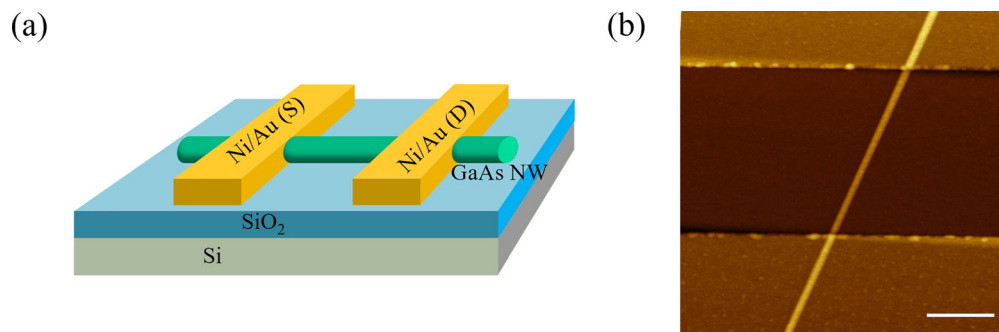
FIG. 1. Schematic device structure and AFM characterization result. (a) Schematic image of a single GaAs nanowire device. (b) AFM image of a single passivated GaAs nanowire device. Scale bar is 2 μm.
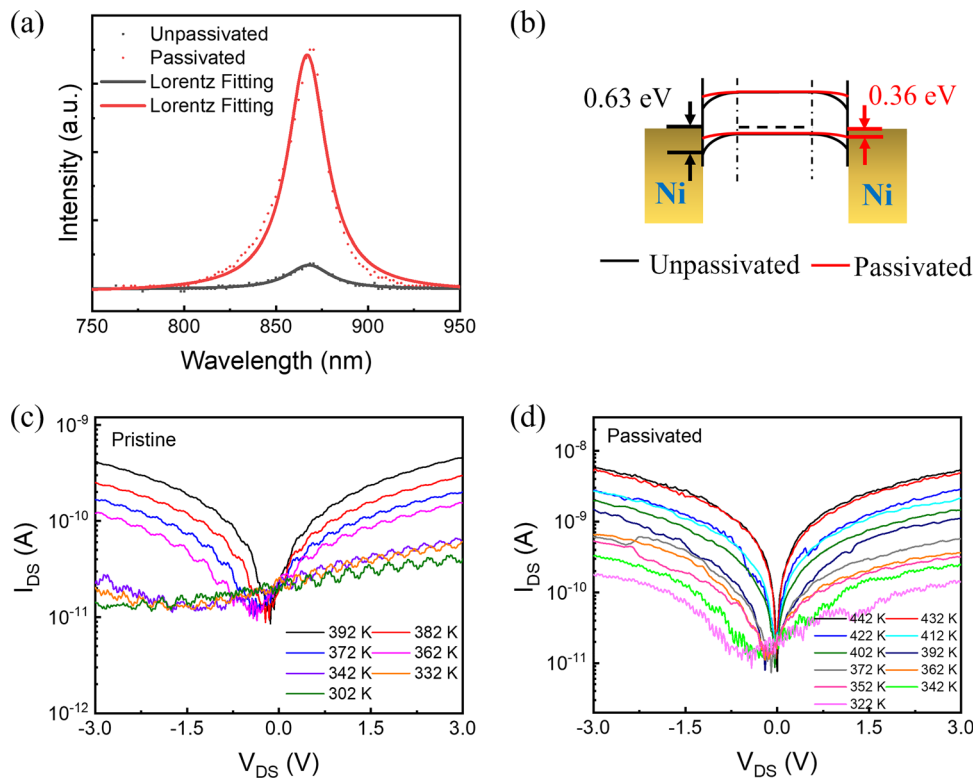
FIG. 2. PL spectra, schematic energy band diagram, and current-voltage relationship of GaAs nanowire devices. (a) PL spectra of pristine and passivated GaAs NWs. (b) Schematic energy band diagram in the dark with energy band bending without and after passivation plotted in black and red, respectively. The currents of the GaAs nanowire devices at different temperatures in the (c) pristine device and (d) passivated device.

I_{DS}-V_{DS} curves measured under darkness and 520 nm laser illumination are shown in Fig. 3(b), where the observed nonlinear relationship was similar to previous MSM photodetectors.[34,35] To verify the Schottky contact between Ni and GaAs nanowires, the spatial image of the photocurrent by raster scanning the laser spot over the device was measured at a bias voltage of 2 V, which is displayed in the inset of Fig. 3(b). The corresponding optical image of the device is shown in Fig. S5. The device exhibited significant photocurrent near the area of contact in a reverse bias, and the asymmetric photocurrent generation indicated the formation of the Schottky contact. The passivated GaAs nanowire device exhibited distinct photoresponse owing to the direct bandgap transition and the optimized design, and the current was 9.3 times larger than that of the pristine device under the same power density of 7 mW cm^{-2} [Fig. S6(a)]. The photoresponse on/off ratio was 625.7 at 2 V bias voltage (520 nm and 24.5 mW cm^{-2}). Additionally, the photocurrent I_{Ph} vs power density was evaluated from the corresponding I-V curves, as shown in Fig. S7. By fitting the scattered dots with the power law function ($I_{Ph} \propto P^{\alpha}$, where α is the exponent),[24] the photodetector after surface passivation presented an improved exponent of 0.69 at $V_{DS} = 2$ V, in comparison to 0.64 in the pristine GaAs nanowire-based device [Fig. S6(b)]. The non-unity α was likely related to the surface states participating in the charge trapping process.[36–38] Similar photoresponse performance was observed under 405, 635, and 780 nm laser illumination (Figs. S8 and S9). The power exponents under illumination at different wavelengths are summarized in

Fig. S10, where it can be commonly observed that higher exponents were acquired at elevated bias voltages with the maximum exponent values distinguished upon 520 nm laser illumination.

It has been observed that in a single GaAs nanowire with diameter above 150 nm lying horizontally on the glass substrate, the external quantum efficiency (EQE)/internal quantum efficiency (IQE) under AM1.5G spectral illumination from the top is on the order of 0.5.[39] Although the intrinsic absorption for the GaAs nanowire may vary depending on the incident wavelength from 405 to 780 nm, the order of magnitude is the same.[1] Therefore, the effective area A_{eff} was estimated to be half of the geometric cross section of the wire exposed to the incident light. The responsivity (R) and specific detectivity (D*) vs the power densities under illumination wavelengths ranging from 405 to 780 nm are plotted in Figs. 3(c) and S11(a), respectively. The data measured at different bias voltages can be found in Figs. S12 and S13. Both figures-of-merit decreased with increasing power density, and the best R and D* were as large as 4.5×10^4 A W^{-1} and 3.3×10^{14} Jones, respectively, upon 520 nm light excitation with a power intensity of 11.5 μW cm^{-2}. Notably, the maximum values of R and D* were both much higher than the ones reported in earlier works for GaAs NW-based MSM photodetectors (R = 2.7 A W^{-1} and D* = 1.35×10^{11} Jones at 0.38 mW cm^{-2})[35] and sulfur passivated GaAs nanowire photodetectors (R = 25 A W^{-1} and D* = 9.04×10^{12} Jones at 2.39 mW cm^{-2})[24] with Cr/Au as the metal contact.[24] Subjecting to the same power density of 7 mW cm^{-2}, the R and D* were both
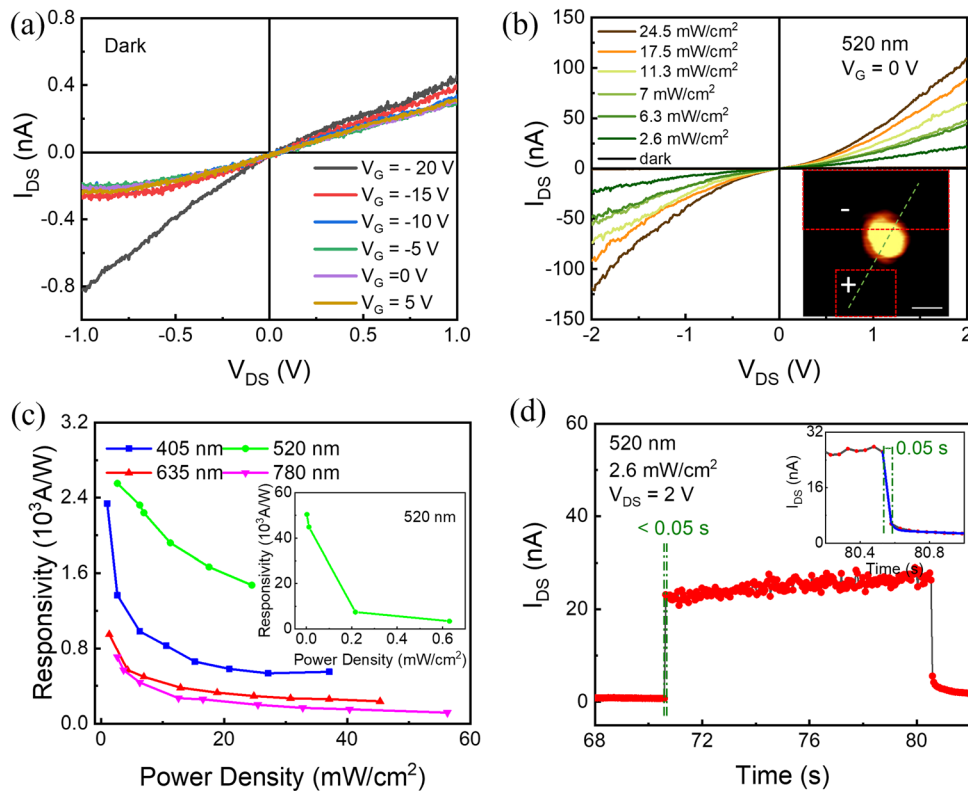
FIG. 3. Photoresponse characteristics of the passivated intrinsic GaAs nanowire-based photodetector. (a) Output curves under darkness. (b) The I_{DS}-V_{DS} relationship in the dark and under various densities at 520 nm laser illumination. Inset shows the spatial image of the photocurrent obtained by raster scanning the laser spot over the passivated GaAs nanowire device. The red dotted lines represent contacts areas, and the green dotted line indicates the position of the nanowire. The bias polarities are indicated. The scale bar is 2 μm. (c) Responsivity as a function of the incident illumination density at 2 V bias voltage. Inset shows R measured under weak light. (d) High-resolution temporal photoresponse. Inset shows the zoom-in recovery process.

improved significantly after surface passivation compared with the results in Fig. S6(c), reaching up to 11.5-fold and threefold values of the pristine device, respectively. The EQE can be calculated by the equation $EQE = Rhc/e\lambda * 100\%$,[37] where c represents the speed of light and λ is the incident light wavelength. The dependence of EQE on power density for illumination with various wavelengths illustrated in Fig. S11(b) showed an analogous trend to the dependence of R on the power density, and it reached $1.1 \times 10^7\%$ under 520 nm illumination, a power density of 11.5 μW cm^{-2}. The high gain could be caused by localized states greatly prolonging the releasing process of trapped carriers for recombination.[40]

As for the wavelength-dependent properties, evidently, the GaAs nanowire photodetector responded to the 520 nm (780 nm) illumination most effectively (least effectively). The current upon 520 nm illumination was 5.4 times higher than that for 780 nm illumination, as shown in Fig. S14, with the same power density of 6.3 mW cm^{-2}. The peak value appearing at 520 nm matched with the typical GaAs spectral photoresponse and the previous simulation results utilizing the Boltzmann transport model.[1,14]

The periodic photocurrent transient measurements were conducted under different illumination power densities (Fig. S15), exhibiting reproducible on/off switching behavior with good stability. In the

magnified time-resolved transient photoresponse upon 520 nm laser illumination depicted in Fig. 3(d), in contrast to the slow response of the pristine device [Fig. S6(d)], the rising time (t_{rise}) was drastically reduced to less than 50 ms. The significantly shortened response time was indicative of much more efficient charge extraction after the passivation treatment. The falling time (t_{fall}) was determined as 50 ms. Also, the rising time less than 50 ms was obtained upon 405, 630 nm and 780 laser illuminations [Figs. S16(a)–S16(c)].

Furthermore, the beryllium-doped GaAs nanowire devices were also subject to the sulfur passivation. With effective doping, the Fermi level of the GaAs nanowire is dragged downwards to the valence band, which narrows the width of the Schottky barrier region. Accordingly, it increases the built-in electrical field and contributes to more efficient photoexcited carriers collection.[35,37] The power-dependent characteristics were obtained under 520 nm illumination, as displayed in Fig. 4(a), and photocurrent and responsivity are shown in Fig. 4(b). Especially, at the power density of 7 mW cm^{-2}, the responsivity improved over 50 times compared with the value that was observed without surface treatment (Fig. S17), being increased as high as 6.4×10^5 A/W. The D* and EQE of the passivated doped device are illustrated in Fig. S18a, showing the peak values of 8.2×10^{12} Jones and $1.5 \times 10^8\%$, respectively. In time-resolved transient photoresponse
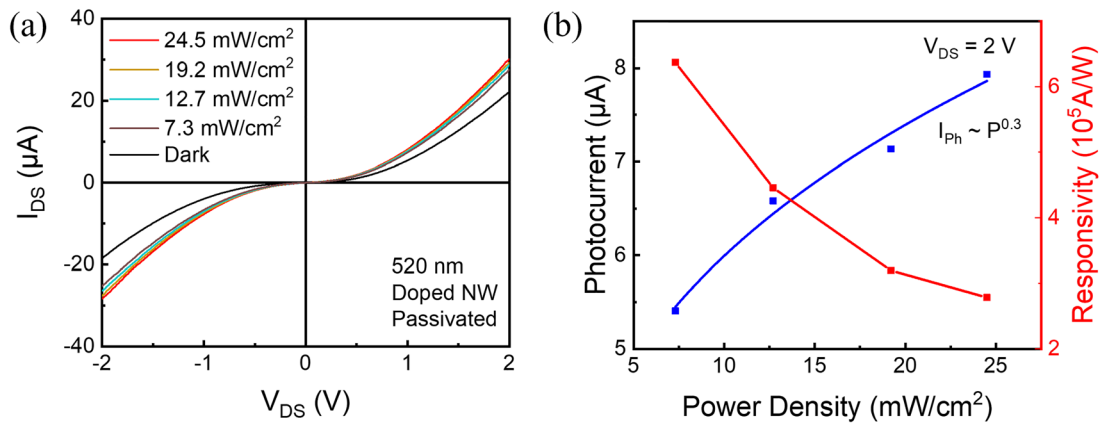
FIG. 4. Photoresponse characteristics of the passivated doped GaAs nanowire-based photodetector. (a) The I_{DS}-V_{DS} relationship in the dark and under 520 nm laser illumination. (b) Dependence of the photocurrent and responsivity on incident illumination density at 2 V bias voltage.

depicted in Fig. S18b, the slow response speed was similar to previously reported result in the doped NW device,[37] which could stem from the impact of carrier scattering that derives from collisions between carriers and lattice defects in the doped GaAs nanowire.[41]

To evaluate the reliability of the passivation effects on GaAs NWs, the performance of the realized devices was statistically analyzed. Overall, the responsivities of eight passivated and seven pristine intrinsic GaAs nanowire-based photodetectors are presented
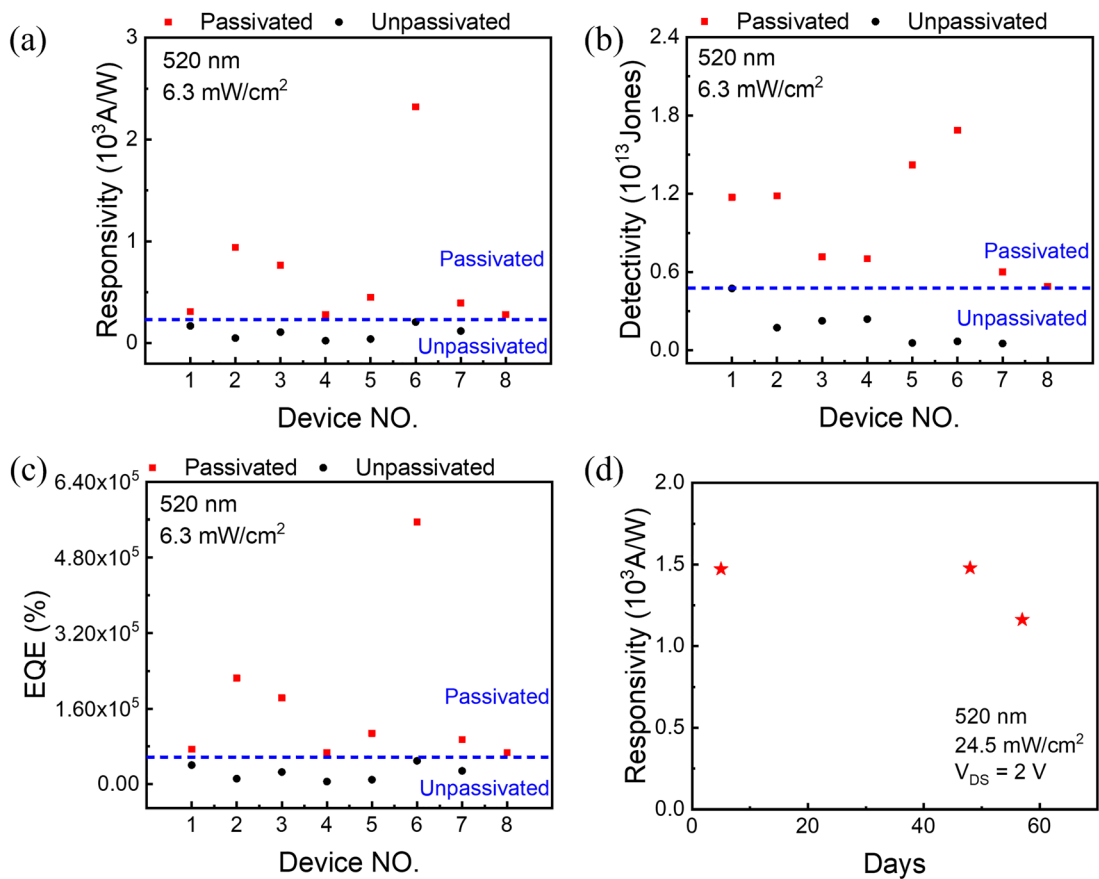
FIG. 5. The photoresponse comparisons of (a) responsivity, (b) specific detectivity, and (c) EQE of eight passivated and seven pristine intrinsic GaAs nanowire-based photodetectors. All devices were measured at $V_{DS} = 2$ V, under 520 nm laser illumination, with a power density of 6.3 mW cm^{-2}. (d) The stability of the passivated intrinsic device showing responsivity variation upon air exposure.

in Fig. 5(a). It is conspicuously shown that the highest R value of pristine devices was smaller than the lowest value of the passivated photodetectors, unambiguously verifying the improved performance of the passivated devices. The average value of the responsivity was 718.2 A W^{-1} (102.3 A W^{-1}) for the passivated (pristine) devices with the efficient surface passivation and reduced Schottky barrier height leading to a sevenfold improvement. Additionally, the D* and the EQE are presented in Figs. 5(b) and 5(c), respectively, showing similar tendencies as R. Likewise, the lowest D* and EQE values for the passivated photodetector of 4.9×10^{12} Jones and 6.7×10^4% were both higher than the peak values for the pristine device of 4.7×10^{12} Jones and 5×10^4%, respectively. To further improve the reproducible manufacturing of the optimized device, the effective contact area of devices, length and width of NWs will need optimization.[42] Furthermore, in order to inspect the stability of the passivated device, the responsivity of the optimized device as a function of the number of days of air exposure is presented in Fig. 5(d). As clearly observed, the R dropped to 78.9% of the as-fabricated device two months later. These results indicated that the hybrid surface and contact optimization improved the photoresponse with good reliability and reproducibility.

For a straightforward assessment, the figures-of-merit related to the performance of GaAs nanowire-based photodetectors that have been reported so far are summarized in Table S1. Importantly, the peak responsivity (at 2 V bias voltage) of the designed passivated photodetector especially after doping is among the highest values of the GaAs nanowire-based photodetectors that have been studied, while it is remarkable that the intrinsic device keeps fast response speed.

To conclude, photodetectors based on high-quality GaAs NWs were demonstrated, and distinct photoresponse improvement was achieved, which was attributed to the synergy of the decreased surface recombination via passivation and the optimized interfacial contact. The passivated intrinsic photodetector exhibited enhanced photoresponse performance, including 11.5-fold higher photosensitivity and much shortened response time in a MSM structure configuration. Specifically, the optimized intrinsic device demonstrated extraordinary characteristics with the high responsivity of 4.5×10^4 A W^{-1}, specific detectivity of 3.3×10^{14} Jones, impressive EQE of 1.1×10^7%, and short rising time less than 50 ms, falling time of 50 ms, and on/off ratio up to 625.7 with 520 nm laser excitation. Additionally, the wavelength-dependent photoresponse revealed the passivated GaAs nanowire device responded to the 520 nm laser illumination most effectively. The responsivity was also enhanced by more than 50 times in the passivated doped GaAs nanowire device, compared to the untreated counterpart, up to 6.4×10^5 A/W. Moreover, the performance enhancement of passivated devices was reliable, and the responsivity of the passivated device was examined to last two months with slight degradation. Through our studies, the great potential of GaAs NWs for high-performance and reliable optoelectronic applications in the nanoscale is demonstrated, which renders the structures promising as one of the essential building blocks for nanophononics. More importantly, the explored route taking both the impact of surface and contact into account could be easily extended to photodetectors based on other materials for the significant enhancement of the photoresponse performance.

See the supplementary material for the experimental methods of nanowire growth, characterizations, device fabrication, and device measurements. Additional AFM, SEM, and optical images of the passivated and pristine nanowire devices, the relationship of slope and bias voltage for barrier heights extraction, transfer characteristic of the passivated device, photoresponse performance of the intrinsic GaAs NW device without treatment, current and photocurrent of the optimized passivated device under laser illumination of other wavelengths, detailed responsivity and specific detectivity at different bias voltages of the optimized passivated device, transient photoresponse of the optimized GaAs nanowire photodetector at 405, 520, 635, and 780 nm laser illumination, the photoresponse performance of the Be-doped GaAs nanowire device without treatment, and the D* and EQE of the passivated doped GaAs nanowire device.

DATA AVAILABILITY

The data that support the findings of this study are available from the corresponding authors upon reasonable request.

REFERENCES

[1]X. Dai, S. Zhang, Z. Wang, G. Adamo, H. Liu, Y. Huang, C. Couteau, and C. Soci, Nano Lett. **14**, 2688 (2014).
[2]H. Wang, Appl. Phys. Lett. **103**, 093101 (2013).
[3]J. V. Holm, H. I. Jørgensen, P. Krogstrup, J. Nygård, H. Liu, and M. Aagesen, Nat. Commun. **4**, 1498 (2013).
[4]P. Krogstrup, H. I. Jørgensen, M. Heiss, O. Demichel, J. V. Holm, M. Aagesen, J. Nygard, and A. Fontcuberta I Morral, Nat. Photonics **7**, 306 (2013).
[5]D. Saxena, S. Mokkapati, P. Parkinson, N. Jiang, Q. Gao, H. H. Tan, and C. Jagadish, Nat. Photonics **7**, 963 (2013).
[6]J. Ho, J. Tatebayashi, S. Sergent, C. F. Fong, S. Iwamoto, and Y. Arakawa, ACS Photonics **2**, 165 (2015).
[7]K. Tomioka, J. Motohisa, S. Hara, K. Hiruma, and T. Fukui, Nano Lett. **10**, 1639 (2010).
[8]R. Yan, D. Gargas, and P. Yang, Nat. Photonics **3**, 569 (2009).
[9]M. Heurlin, Z. Bi, B. Monemar, L. Samuelson, E. Barrigo, and S. V. Ab, Chem. Rev. **119**, 9170 (2019).
[10]R. R. Lapierre, M. Robson, K. M. Azizur-Rahman, and P. Kuyanov, J. Phys. D: Appl. Phys. **50**, 123001 (2017).
[11]X. Gan, R. J. Shiue, Y. Gao, I. Meric, T. F. Heinz, K. Shepard, J. Hone, S. Assefa, and D. Englund, Nat. Photonics **7**, 883 (2013).
[12]Y. Liu, F. Wang, X. Wang, X. Wang, E. Flahaut, X. Liu, Y. Li, X. Wang, Y. Xu, Y. Shi, and R. Zhang, Nat. Commun. **6**, 8589 (2015).
[13]G. Konstantatos, M. Badioli, L. Gaudreau, J. Osmond, M. Bernechea, F. P. G. De Arquer, F. Gatti, and F. H. L. Koppens, Nat. Nanotechnol. **7**, 363 (2012).
[14]L. Zhang, X. Geng, G. Zha, J. Xu, S. Wei, B. Ma, Z. Chen, X. Shang, H. Ni, and Z. Niu, Mater. Sci. Semicond. Process. **52**, 68 (2016).
[15]S. Thunich, L. Prechtel, D. Spirkoska, G. Abstreiter, A. Fontcuberta I Morral, and A. W. Holleitner, Appl. Phys. Lett. **95**, 083111 (2009).
[16]E. M. Gallo, G. Chen, M. Currie, T. McGuckin, P. Prete, N. Lovergine, B. Nabet, and J. E. Spanier, Appl. Phys. Lett. **98**, 241113 (2011).
[17]J. A. Czaban, D. A. Thompson, and R. R. LaPierre, Nano Lett. **9**, 148 (2009).
[18]M. A. Seyedi, M. Yao, J. O'Brien, S. Y. Wang, and P. D. Dapkus, Appl. Phys. Lett. **103**, 251109 (2013).

[19]Y. Wu, X. Yan, X. Zhang, and X. Ren, Appl. Phys. Lett. **109**, 183101 (2016).

[20]D. Wang, X. Chen, X. Fang, J. Tang, F. Lin, X. Wang, G. Liu, L. Liao, J. C. Ho, and Z. Wei, Nanoscale **13**, 1086 (2021).

[21]X. Chen, B. Jiang, D. Wang, G. Li, H. Wang, H. Wang, F. Wang, P. Wang, L. Liao, and Z. Wei, Appl. Phys. Lett. **118**, 041102 (2021).

[22]H. J. Joyce, C. J. Docherty, Q. Gao, H. H. Tan, C. Jagadish, J. Lloyd-Hughes, L. M. Herz, and M. B. Johnston, Nanotechnology **24**, 214006 (2013).

[23]C. Gutsche, R. Niepelt, M. Gnauck, A. Lysov, W. Prost, C. Ronning, and F. J. Tegude, Nano Lett. **12**, 1453 (2012).

[24]X. Chen, N. Xia, Z. Yang, F. Gong, Z. Wei, D. Wang, J. Tang, X. Fang, D. Fang, and L. Liao, Nanotechnology **29**, 095201 (2018).

[25]C. C. Chang, C. Y. Chi, M. Yao, N. Huang, C. C. Chen, J. Theiss, A. W. Bushmaker, S. Lalumondiere, T. W. Yeh, M. L. Povinelli, C. Zhou, P. D. Dapkus, and S. B. Cronin, Nano Lett. **12**, 4484 (2012).

[26]N. Tajik, A. C. E. Chia, and R. R. Lapierre, Appl. Phys. Lett. **100**, 203122 (2012).

[27]P. A. Alekseev, M. S. Dunaevskiy, V. P. Ulin, T. V. Lvova, D. O. Filatov, A. V. Nezhdanov, A. I. Mashin, and V. L. Berkovits, Nano Lett. **15**, 63 (2015).

[28]Z. Li, X. Yuan, Q. Gao, I. Yang, L. Li, P. Caroff, M. Allen, J. Allen, H. H. Tan, C. Jagadish, and L. Fu, Nanotechnology **31**, 244002 (2020).

[29]J. Miao, W. Hu, N. Guo, Z. Lu, X. Zou, L. Liao, S. Shi, P. Chen, Z. Fan, J. C. Ho, T. X. Li, X. S. Chen, and W. Lu, ACS Nano **8**, 3628 (2014).

[30]H. Fang, W. Hu, P. Wang, N. Guo, W. Luo, D. Zheng, F. Gong, M. Luo, H. Tian, X. Zhang, C. Luo, X. Wu, P. Chen, L. Liao, A. Pan, X. Chen, and W. Lu, Nano Lett. **16**, 6416 (2016).

[31]X. Yu, H. Wang, J. Lu, J. Zhao, J. Misuraca, P. Xiong, and S. Von Molnár, Nano Lett. **12**, 5436 (2012).

[32]H. Zeng, X. Yu, H. A. Fonseka, J. A. Gott, M. Tang, Y. Zhang, G. Boras, J. Xu, A. M. Sanchez, and H. Liu, Nano Lett. **18**, 6397 (2018).

[33]K. K. N. Sze, M. Simon, and Y. Li, *Physics of Semiconductor Devices* (John Wiley & Sons, Inc., 2021).

[34]Y. Gu, E. S. Kwak, J. L. Lensch, and J. E. Allen, Appl. Phys. Lett. **87**, 043111 (2005).

[35]X. Chen, D. Wang, T. Wang, Z. Yang, X. Zou, P. Wang, W. Luo, Q. Li, L. Liao, W. Hu, and Z. Wei, ACS Appl. Mater. Interfaces **11**, 33188 (2019).

[36]M. Buscema, D. J. Groenendijk, S. I. Blanter, G. A. Steele, H. S. J. Van Der Zant, and A. Castellanos-Gomez, Nano Lett. **14**, 3347 (2014).

[37]H. Ali, Y. Zhang, J. Tang, K. Peng, S. Sun, Y. Sun, F. Song, A. Falak, S. Wu, C. Qian, M. Wang, Z. Zuo, K. J. Jin, A. M. Sanchez, H. Liu, and X. Xu, Small **14**, 1704429 (2018).

[38]H. Kind, H. Yan, B. Messer, M. Law, and P. Yang, Adv. Mater. **14**, 158 (2002).

[39]M. Heiss, A. Fontcuberta, and I. Morral, Appl. Phys. Lett. **99**, 263102 (2011).

[40]H. Fang and W. Hu, Adv. Sci. **4**, 1700323 (2017).

[41]X. Zhu, F. Lin, Z. Zhang, X. Chen, H. Huang, D. Wang, J. Tang, X. Fang, D. Fang, J. C. Ho, L. Liao, and Z. Wei, Nano Lett. **20**, 2654 (2020).

[42]D. K. Schroder, *Contact Resistance and Schottky Barriers* (Wiley-IEEE Press, 2006).